

Molecular characterization of the sodium channel subunits expressed in mammalian cerebellar Purkinje cells

(cerebellum/persistent Na⁺ channel)

ELEAZAR VEGA-SAENZ DE MIERA*, BERNARDO RUDY*†, MUTSUYUKI SUGIMORI*, AND RODOLFO LLINÁS*‡

*Department of Physiology and Neuroscience and †Department of Biochemistry, New York University Medical Center, 550 First Avenue, New York, NY 10016

Contributed by Rodolfo Llinás, April 15, 1997

ABSTRACT Inactivating and noninactivating Na⁺ conductances are known to generate, respectively, the rising phase and the prolonged plateau phase of cerebellar Purkinje cell (PC) action potentials. These conductances have different voltage activation levels, suggesting the possibility that two distinct types of ion channels are involved. Single Purkinje cell reverse transcription–PCR from guinea pig cerebellar slices identified two Na⁺ channel α subunit transcripts, the orthologs of RBI (rat brain I) and Nach6/Scn8a. The latter we shall name CerIII. *In situ* hybridization histochemistry in rat brain demonstrated broad CerIII expression at high levels in many neuronal groups in the brain and spinal cord, with little if any expression in white matter, or nerve tracts. RBII (rat brain II), the most commonly studied recombinant Na⁺ channel α subunit is not expressed in PCs. As the absence of Scn8a has been correlated with motor endplate disease (med), in which transient sodium currents are spared, RBI appears to be responsible for the transient sodium current in PC. Conversely, jolting mice with a mutated Scn8a message demonstrates PC abnormalities in rapid, simple spike generation, linking CerIII to the persistent sodium current.

The electrical activity of excitable tissues is mediated by voltage- and ligand-gated ion channels. Purkinje cells express at least two different voltage-gated sodium conductances, one responsible for the fast depolarization phase of the action potential and the second for the prolonged plateau potentials (1). This latter current activates at more negative potentials (2). Noninactivating Na⁺ conductances are also seen in other neurons (3–6) and play an important role in neuronal oscillatory properties (7, 8).

Eleven different genes that encode subunits of voltage-gated Na⁺ channels have been identified in mammals (9–23). Of these, eight are expressed in the nervous system (11, 22–25); two of these are also expressed in heart and denervated skeletal muscle (11, 14).

Biochemical studies have shown that voltage-gated sodium channels are composed of a large (230 to 270 kDa) subunit and several smaller subunits (26–28). The biophysical characteristics of the I_{Na} supported by the large subunit is significantly modulated by its associated subunits (28, 29) and its phosphorylation status (30–32).

To determine whether the transient and maintained Na⁺ conductances in PCs could be supported by different sodium channels, the Na⁺ channel α subunit transcripts expressed in these cells were studied using single-cell reverse transcription–PCR (RT-PCR). Part of these results have been presented in abstract form (33).

The publication costs of this article were defrayed in part by page charge payment. This article must therefore be hereby marked “advertisement” in accordance with 18 U.S.C. §1734 solely to indicate this fact.

© 1997 by The National Academy of Sciences 0027-8424/97/947059-6\$2.00/0

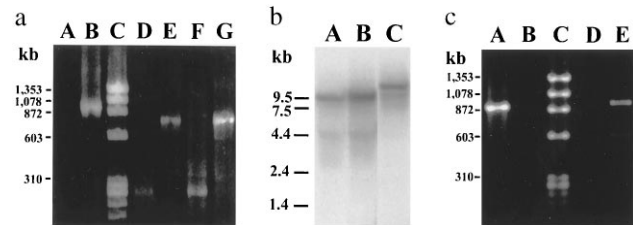


FIG. 1. Expression of Na channel α subunits mRNAs in cerebellum. (a) PCR amplification of sodium channel sequences in genomic DNA and cerebellar rRNA. Two percent agarose gel. Genomic DNA (100 ng) or rRNA (40 ng) was subjected to 40 cycles of PCR amplification under standard PCR conditions. Lanes: A, no rRNA or DNA (negative control); B, cerebellar rRNA; C, ϕ 174 HaeIII Std.; D, rat genomic DNA with the primers directed to sodium channels; E, rat genomic DNA with primers that amplify a 740-bp product in genomic DNA (positive control); F and G, similar to D and E but with genomic DNA from mice. (b) Expression of sodium channels in rat cerebellar mRNA. Northern blots of rat cerebellar poly(A) RNA (4 μ g per lane) were hybridized with probes specific to RBI (A), RBII (B), or CerIII (C). The blots were exposed to Kodak XAR-5 film at -70°C with no intensifying screens. The RNA sizes are from GIBCO/BRL RNA markers. (c) Single-cell RT-PCR. Samples obtained throughout the recording electrodes from a single cell were amplified by PCR with Na⁺ channel-specific degenerate oligonucleotides. Seven microliters of the amplification reaction were run in 2% agarose gel. Lanes: A, 50 ng of reverse-transcribed cerebellar RNA; B, chamber solution in presence of reverse transcriptase (control 1); C, ϕ 174-HaeIII molecular weight Std.; D, non-reverse-transcribed RNA from a single PC (control 2); E, reverse-transcribed RNA from a single Purkinje cell.

MATERIALS AND METHODS

Single-Cell RT-PCR. Single-cell RT-PCR was performed as described by Lambolez *et al.* (34). All materials were freed of RNase by heating at 160°C or soaking in 3% H₂O₂ for 10 min. Solutions were made in double-distilled water from GIBCO/BRL.

The electrodes were filled with recording solution containing 120 mM CsCl, 3 mM MgCl₂, and 5 mM EGTA and 10 mM HEPES, pH 7.2. The reverse transcriptase master-mix solution included 1.67 mM dNTP, 4.17 mM MgCl₂, 4,000 units per ml of Moloney Murine Leukemia Virus RNase H⁻ reverse transcriptase, 6.25 μ M random hexamer primer, 1,667 units per ml of RNase inhibitor. The PCR master-mix solution included 26.7 mM KCl, 0.66 mM MgCl₂, 1.7 μ M of the sense and antisense primers, and 5.33 mM Tris-HCl, pH 8.3. *Taq* polymerase enzyme mix included 24 mM KCl, 0.60 mM MgCl₂, 500 units per ml *Taq* polymerase, and 4.8 mM Tris-HCl, pH 8.3.

Abbreviations: PC, Purkinje cell; RT-PCR, reverse transcription–PCR; RBI and II, rat brain I and II, respectively. Data deposition: The sequences reported in this paper have been deposited in the GenBank database [accession nos. AF003372 (GpBI) and AF003373 (CerIII)].

‡To whom reprint requests should be addressed.

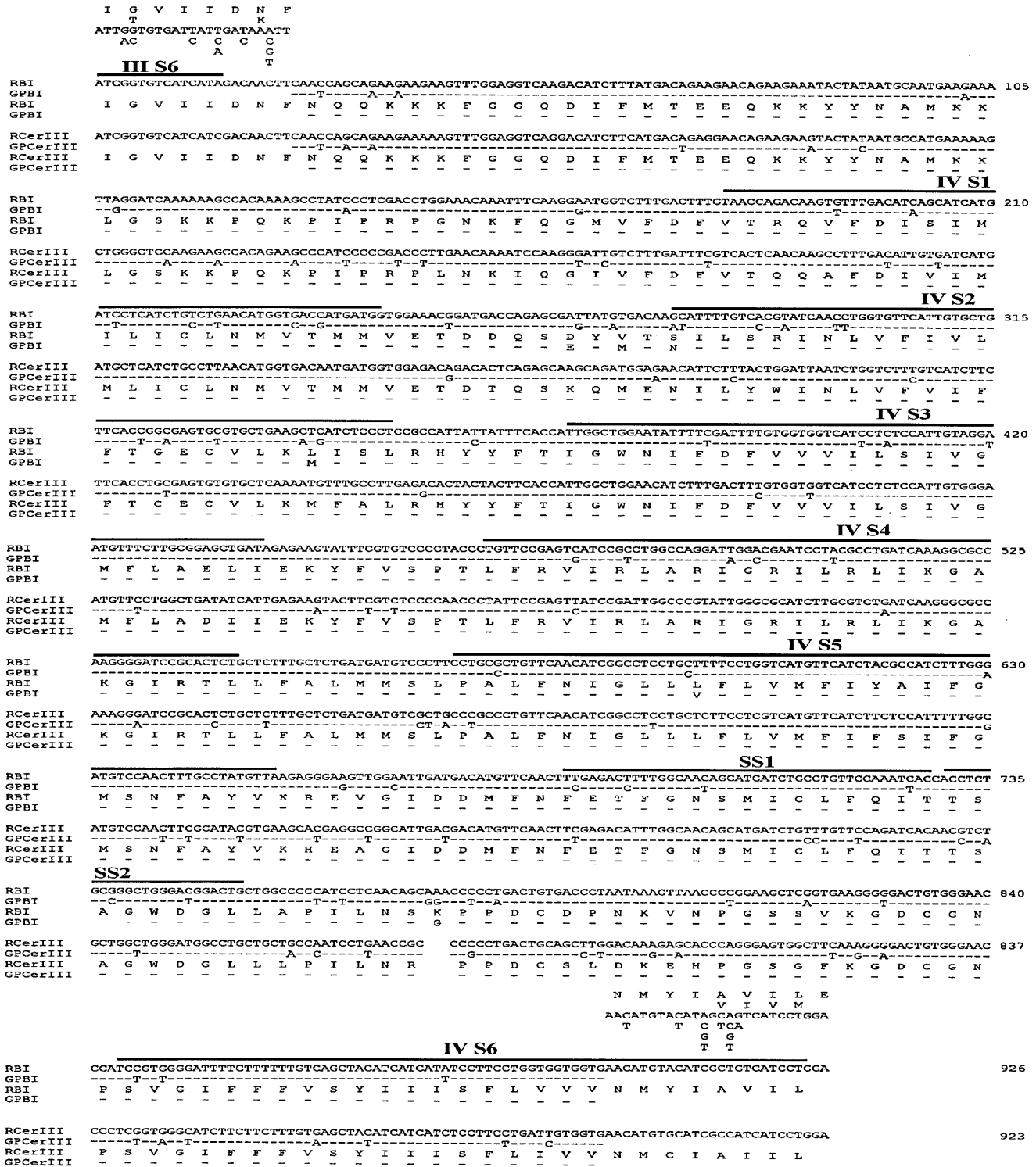


FIG. 2. Alignment of sodium channel sequences isolated from single cerebellar Purkinje cells by RT-PCR. Nucleotide and deduced amino acid sequence of the sodium channel sequences isolated by single-cell PCR from guinea pig cerebellar Purkinje cell, compared with their rat ortologs. A dash represents identical nucleotide or amino acid in that position.

Primer Design. Oligonucleotides matching the S6 region of the third and fourth repeats flanking a stretch of 924 nucleotides of known sodium channel α subunits (12, 13, 15–19, 21, 35–39) were designed (40). The sense oligonucleotide ATT GGT/C GTT/C ATT/C ATT/C/A GAT/C AAN TT is a 23-mer with a degeneracy of 144, and the antisense oligonucleotide TC CAG GAT GAC/T NG/AC A/G/TAT G/ATA CAT G/ATT, a 27-mer with a degeneracy of 192.

RNA Collection, Reverse Transcription, and PCR. RNA from single guinea pig Purkinje cells was obtained using

recording microelectrodes filled with 8 μ l of recording solution. The electrodes were emptied into 0.5-ml Ependorf tubes and subjected to reverse transcription as follows: 12 μ l of reverse transcriptase master mix was added to the tube and 50 μ l of oil was laid over, the tubes were incubated for 10 min at 20°C, followed by 15 min at 42°C and 5 min at 99°C, and then cooled to 5°C for 5 min. PCR solution mix (75 μ l) was added to the cDNA, the mixture was heated for 5 min at 94°C, 5 μ l *Taq* solution was added, and 45 cycles of PCR were applied [1 min annealing at 48°C (except the first two annealing cycles

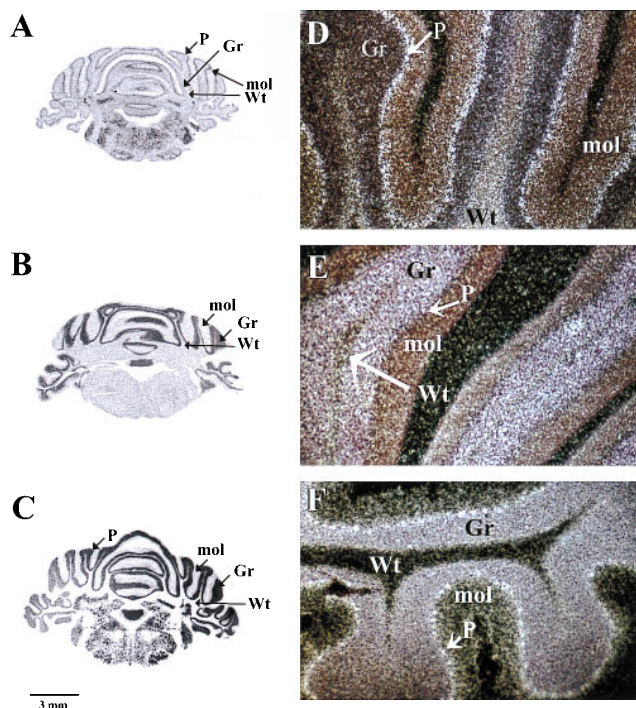


FIG. 3. Expression of RbI, RbII, and CerIII sodium channel mRNA in cerebellum. X-ray film autoradiograms of coronal sections A–C and their corresponding dark field images from emulsion autoradiograms D–F. A and D, B and E, and C and F hybridized to RbI, RbII, and CerIII sodium channel probes, respectively.

that were at 45°C), 1 min extension at 72°C, and 1 min denaturing at 94°C]. RT-PCR from cerebellar tissue was performed in a similar way to the single-cell RT-PCR except that 50 ng of total cerebellar RNA was used instead of the Purkinje cell RNA. The bands obtained from the RT-PCR were gel purified using Schleicher & Schuell NA45 DEAE-paper, ligated into T-tailed *Sma*I cut pBluescript (41), and sequenced by the dideoxisequencing method (42) using Sequenase (United States Biochemical).

Probes for Northern Blot Analysis and *in Situ* Hybridization. Probes were prepared by labeling cDNA fragments using the random hexamer primer method (43) with ^{32}P or ^{35}S (for Northern blots and *in situ* hybridization, respectively). The following fragments were used: RbI, 638 bp from nucleotides 5952–6598 (17); RbII, 650 bp from nucleotides 5874–6524 (18); and CerIII (the first 523 nucleotides of the clone isolated from the cerebellar RT-PCR).

Preparation of RNA and Northern Blot Analysis. Total RNA from adult (150–175 g) Sprague-Dawley rat cerebellum was prepared using the guanidinium-thiocyanate method (44), and poly(A) was selected with oligo(dT) cellulose columns as previously described (45). The RNA was electrophoresed in formaldehyde-denaturing gels and transferred to Hybond N (Amersham) (45). The blots were hybridized with 1×10^6 cpm TCA precipitable counts (0.5 to 1.0 ng of DNA/ml) of ^{32}P -labeled probes per ml at 68°C in Stratagene Quick Hib for 2 h. After hybridization the blots were washed twice at room temperature in $2 \times \text{SSC}$ with 0.1% SDS for 15 min, and then washed for 30 min at 60°C in $0.1 \times \text{SSC}$ with 0.1% SDS. The blot was exposed overnight at -70°C without intensifying screens.

***In Situ* Hybridization.** Rat brain sections were hybridized with ^{35}S -labeled probes as previously described by Stone *et al.* (46). Briefly, the rats were deeply anesthetized with sodium pentobarbital (Nembutal; 90 mg/kg, i.p.) and perfused transcardially with normal saline containing 0.5% NaNO_2 and 10 units per ml of heparin followed by 400 ml of ice-cooled 0.1 M

phosphate buffer (pH 7.2) containing 4% formaldehyde (prepared from paraformaldehyde). The brains were removed, cut in blocks, postfixed for 2–4 h in the 4% formaldehyde solution, and placed in 30% sucrose overnight or until blocks settled. Coronal or sagittal (30–40 μm) freezing microtome sections were collected in scintillation vials containing cold $2 \times \text{SSC}$ made in diethyl-pyrocyanate water. The sections were prehybridized for 1–2 h at 48°C in a 53% formamide solution (1.75 \times SSC/8.8% dextran sulfate/3.5 \times Denhardt's solution/50 mM dithiothreitol/4.4 mM EDTA/44 mM Tris, pH 7.4/1.4 mg/ml sonicated denatured salmon sperm DNA). After prehybridization, denatured labeled probe was added and the sections hybridized for 17 h at 48°C. After hybridization, the sections were washed twice with $2 \times \text{SSC}$ solution at 48°C followed by washing with SSC solutions of decreasing concentration: $1 \times$, $0.5 \times$, $0.25 \times$, and $0.1 \times$ for 15 min at each concentration. The sections were transferred into 0.1 M phosphate buffer, mounted on slides, and air dried. The slides were exposed to Microvision-C (Dupont) film for 2–7 days and then dipped in photographic emulsion (Kodak NTB-2) and stored at 4°C (in the dark) for 6–21 days. After developing in Kodak D-19, the slides were fixed, counterstained with cresyl violet, and coverslipped with Permount (Fisher Scientific). The data were analyzed by dark-field and bright-field microscopy with an Olympus BH2 photomicroscope. Central nervous system neuronal populations were identified using standard anatomical references (47–49).

RESULTS

The PCR Target Sequence Is Not Contiguous in the Genome. The primers designed to identify sodium channel α subunit transcripts did not amplify the expected products when genomic DNA was used (Fig. 1a, lanes D and F), but were able to amplify cerebellar rtRNA (Fig. 1a, lane B). The lack of amplification from genomic DNA was not due to the quality of the DNA because a fragment of 764 bp of exon III of Kv3 potassium channels was amplified (50). This suggests that the sequence spanned by the primers is not contiguous in the genome. In sodium channel α subunit genes with known genomic organization, the sequence that is amplified from mRNA transcripts is derived from four different exons (39, 51–53).

Three Different Sodium Channel α Subunits Are Expressed in Cerebellum. Twenty-seven individual isolates from two independent amplifications from cerebellar rtRNA were sequenced. Three different sodium channel α subunits sequences were found: Rat Brain I (RbI), Rat Brain II (RbII), and CerIII. Northern blot analysis of poly(A) cerebellar RNA shows the typical bands for RbI (Fig. 1b, lane A) and RbII (Fig. 1b, lane B), and a weak ≈ 10 -kb band and a strong band of ≈ 12 kb for CerIII (Fig. 1b, lane C).

Cerebellar Purkinje Cells Expressed Two Different Sodium Channels. PCR-generated bands from rtRNA derived from single PC (Fig. 1c, lane E) were subcloned, and individual clones were sequenced. Two different sequences were found; one was identified as the guinea pig ortholog of rat brain I (98% identity) and the other one the guinea pig ortholog of CerIII (100% identity) (Fig. 2). *In situ* hybridization experiments in rat brains showed that RbI and CerIII are expressed in Purkinje cells (Fig. 3 D and F, respectively). RbI was also expressed in deep cerebellar nuclei and weakly in the granular cell layer (Fig. 3 A and D). RbII, the most commonly studied isoform in heterologous expression systems, was expressed strongly in the granular cell layer but has no detectable expression on cerebellar Purkinje cells (Fig. 3 B and E). CerIII was strongly expressed in granule and Purkinje cells and was strongly expressed in the molecular cell layer. The signal in cerebellar white matter was similar to background. Deep

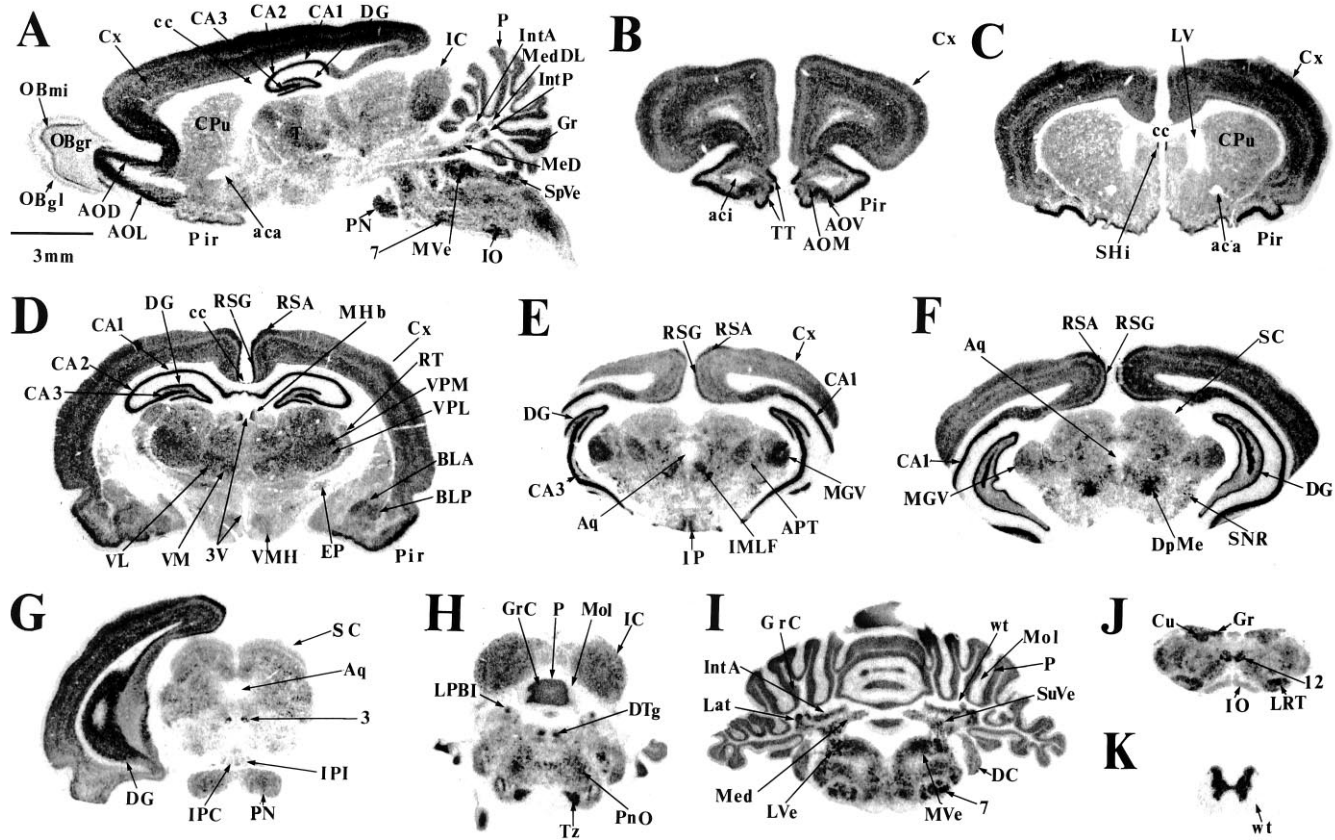


FIG. 4. Expression of CerIII mRNA in the central nervous system. Autoradiograph of sagittal (A) and coronal sections at different levels (B–K) of rat central nervous system hybridized with rat CerIII probe. 3, oculomotor nucleus; 3V, third ventricle; 7, facial nucleus; 12 and 12n, hypoglossal nucleus and nerve, respectively; aca, anterior commissure anterior; aci, anterior commissure interstitial; AOD, anterior olfactory dorsal nucleus; AOL, anterior olfactory lateral nucleus; AOM, anterior olfactory medial nucleus; AOV, anterior olfactory ventral nucleus; APT, anterior pretectal nucleus; Aq, aqueduct; BLA, anterior basolateral amygdaloid nucleus; BLP, posterior basolateral amygdaloid nucleus; CA1 to CA3, areas of Ammon's horn; cc, corpus callosum; CPu, caudate putamen; Cu, cuneatus nucleus; Cx, cortex; DC, dorsal cochlear nucleus; DG, dentate gyrus; DpMe, deep mesencephalic nucleus; DTg, dorsal tegmental nucleus; EP, entopeduncular nucleus; EP, entopeduncular nucleus; Gr, cerebellar granule cell layer; GrC, cerebellar granule cell layer; IC, inferior colliculus; IMLF, interstitial nucleus of the medial longitudinal fasciculus; IntA, anterior interposed nucleus; IntP, posterior interposed nucleus; IO, inferior olive; IP, interpeduncular nucleus; IPC, caudal interpeduncular nucleus; IPI, intermediate interpeduncular nucleus; Lat, lateral cerebellar nucleus (dentate nucleus); LPBI, lateral part of the lateral parabrachial nucleus; LRT, lateral reticular nucleus; LV, lateral ventricle; LVe, lateral vestibular nucleus; Med, medial cerebellar nucleus; MeD, dorsal medial cerebellar nucleus; MedDL, dorsolateral subdivision of the medial cerebellar nucleus; MGV, medial geniculate body; MHb, medial habenular nucleus; Mol, cerebellar molecular cell layer; MVe, medial vestibular nucleus; OBgl, olfactory bulb glomerular cell layer; OBgr, olfactory bulb granular cell layer; OBmi, olfactory bulb mitral cell layer; P, cerebellar Purkinje cell layer; Pir, piriform cortex; PN, pontine nucleus; PnO, pontine reticular nucleus, oral; RSA, agranular retrosplenial cortex; RSG, granular retrosplenial cortex; Rt, reticular thalamus; SC, superior colliculus; SHi, septohippocampal nucleus; SNR, substantia nigra reticulata; SpVe, spinal vestibular nucleus; SuVe, superior vestibular nucleus; T, thalamus; TT, tenia tecta; Tz, nucleus of the trapezoid body; VL, ventrolateral nucleus; VM, ventromedial nucleus; VMH, ventromedial hypothalamic nucleus; VPL, ventroposterior lateral nucleus; VPM, ventroposterior medial nucleus; wt, white matter.

cerebellar nuclear cells were also strongly labeled (Fig. 3 C and F).

CerIII Is Broadly Expressed in the Central Nervous System.

In situ hybridization experiments showed that CerIII mRNA was abundant in many neuronal populations of the central nervous system. In the olfactory bulb, signal was found over the glomerular and mitral cell layers, and moderate expression was seen in granular cells. Higher levels of expression were found in anterior, dorsal, lateral (Fig. 4A), and ventral olfactory nuclei (Fig. 4B). In cerebral cortex strong expression was observed displaying a lamellar distribution (Fig. 4A–G). The mRNA was more abundantly expressed in the retrosplenial (Fig. 4D–F) and piriform (Fig. 4A–D) cortex. In these cortical areas the message was highly expressed in layer II (Fig. 5A and C). In the parietal cortex strong labeling was seen in the large neurons of layer V (Fig. 5B). In the hippocampus high levels of expression were observed in CA1–CA3 pyramidal cells (Fig. 4A and D–F and Fig. 5D), in the granule cells, and in some interneurons of the polymorphic layer of the dentate gyrus (Fig. 4A and D–G and Fig. 5D). High levels of expression were

also found in the septo-hippocampal nucleus, while moderate levels of expression were observed in the caudate-putamen (Fig. 4A and C), hypothalamic nuclei, and the reticular thalamus. Stronger signals were found in the medial habenular nucleus and in several thalamic nuclei (VPM, VPL, VL, and VM; Fig. 4D). The CerIII mRNA was also found in the entopeduncular nucleus and in the amygdala. In the latter structure the level of expression was higher in the BLA and BLP nuclei (Fig. 4D). Several midbrain structures also expressed high levels of CerIII mRNA, such as the inferior colliculus, medial geniculate body, anterior pretectal nucleus, the nucleus of the medial longitudinal fasciculus (Fig. 4E), deep mesencephalic nucleus (Fig. 4F), interpeduncular nucleus, and oculomotor nucleus (Fig. 4G). Fewer high levels of expression were observed in the superior colliculus and in substantia nigra reticulata (Fig. 4F). Medium levels of expression were found in the caudal interpeduncular nucleus and the intermediate interpeduncular nucleus (Fig. 4G). The mRNA was highly expressed in the medulla pons region with strong expression in the internal part of the lateral parabrachial

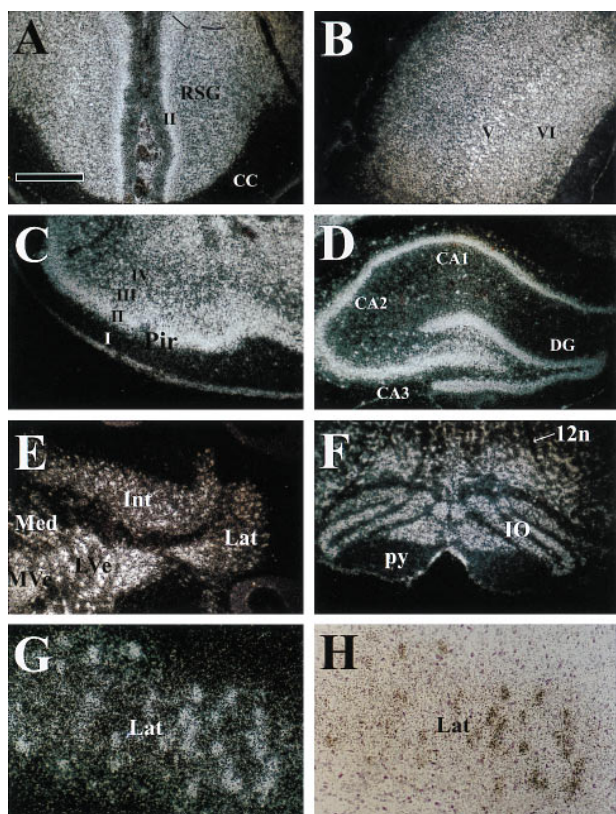


FIG. 5. Dark field images of selected brain areas hybridized with CerIII probe. (A) Retrosplenial granular cortex; (B) cortex; (C) piriform cortex; (D) hippocampus; (E) deep cerebellar nuclei; (F) inferior olive; (G and H) dark field and bright field of the lateral cerebellar nucleus. See Fig. 4 for abbreviations. Scale bar = 0.6 mm for A–F and 0.15 mm for G and H.

nucleus, and in the trapezoid nucleus, dorsal tegmental nucleus (Fig. 4H), pontine nuclei (Fig. 4G), oral part of the pontine reticular nucleus (Fig. 4H), and vestibular nuclei. High levels of expression were also found in all the deep cerebellar nuclei (Figs. 4I and 5E). In these nuclei the mRNA was highly expressed by the large neurons (Fig. 5G and H). High levels of expression were also found in cuneate, gracilis, hypoglossal, facial, and spinal trigeminal nuclei (Fig. 4J), and in the inferior olive (Figs. 4J and 5F). In the spinal cord the mRNA was abundantly expressed in gray matter. Background signals were found over the corpus callosum (Figs. 4A, C, and D, and 5A), cerebellar white matter (Fig. 3C and F), anterior commissure (Fig. 4A–D), and nerve tracts such as the facial (not shown) and hypoglossal nerve bundles (Fig. 5F).

DISCUSSION

mRNA transcripts for three sodium channel α subunits were found by RT-PCR of cerebellum, RbI, RbII, and CerIII. Of this, only RbI and CerIII were expressed in adult Purkinje cells based on single-cell RT-PCR (Figs. 1, 3, and 4) and *in situ* hybridization histochemistry (Fig. 3). We also show that CerIII is mostly a neuronal channel, highly expressed in the brain and spinal cord.

Electrophysiologically, Purkinje cells demonstrate two different sodium conductances, a fast-inactivating and a noninactivating or persistent conductance (1). These have similar single-channel conductance but differ in their voltage-dependence, with the persistent sodium channel activating at potentials negative to those required for the activation of the transient sodium currents (2). Several hypotheses have been proposed to account for the persistent sodium currents: (i) It

represents a window current from the traditional Na conductance (54). However, the theoretical curve does not correspond to the experimental findings (54). (ii) It results from a sodium channel with multiple gating states, where the switching between gating states is voltage-dependent (55). (iii) It is supported by a Na⁺ channel different from that responsible for the transient conductance.

The results presented here, together with recent observations from mutant mice, support the latter hypothesis. Thus, it was found that an insertion in the gene encoding Scn8a produces a med phenotype (56). This finding has been confirmed by demonstrating that med¹ and med result in premature termination of the coding sequence of Scn8a, producing nonfunctional Scn8a channels (57). Electrophysiological studies of med mice show that their Purkinje cells generate abnormally low simple-spike frequency without altering axonal conduction velocity (58). These findings indicate that med Purkinje cells express functional transient sodium channels and, therefore, that RBI encodes such channels.

In contrast to the “jolting” mutant, an allele of med has a defect in Scn8a that causes a positive shift in the voltage dependence of these channels (59). Interestingly, in this mutant, PC fail to generate simple spike trains (58, 60), as would be expected if the persistent sodium conductance functions as a graded spike-boosting system (1). Taken together, the data presented here suggest that RBI mediates the fast, transient conductance and CerIII, the persistent Na current in cerebellar Purkinje cells. However, as neither the RBI nor CerIII subunits have been expressed in heterologous expression systems, the above conclusion must remain tentative. (Such studies will determine whether the special properties of the maintained Na conductance depend on the structure of the large subunit itself or on interactions with β subunits or specific postranslational modifications.)

We thank Joseph Frey for technical assistance. This work was supported by grants from the National Institutes of Health/National Institute of Neurological Diseases and Stroke to R.L. (NS13742) and to B.R. (NS30989).

1. Llinás, R. & Sugimori, M. (1980) *J. Physiol.* **305**, 174–195.
2. Sugimori, M., Kay, A. R. & Llinás, R. (1994) *Soc. Neurosci. Abstr.* **20**, 63.
3. Connors, B. W., Gutnick, M. J. & Prince, P. A. (1982) *J. Neurophysiol.* **48**, 1302–1321.
4. French, C. R. & Gage, P. W. (1985) *Neurosci. Lett.* **56**, 289–293.
5. Schwindt, P. C. & Crill, W. E. (1980) *J. Neurophysiol.* **43**, 1700–1724.
6. Stafstrom, C. E., Schwindt, P. C. & Crill, W. E. (1982) *Brain Res.* **236**, 221–226.
7. Alonso, A. & Llinás, R. (1989) *Nature (London)* **342**, 175–177.
8. Llinás, R., Grace, A. A. & Yarom, Y. (1991) *Proc. Natl. Acad. Sci. USA* **88**, 897–901.
9. Akopian, A. N., Sivilotti, L. & Wood, J. N. (1996) *Nature (London)* **379**, 257–262.
10. Felipe, A., Knittle, J., Doyle, K. L. & Tamkun, M. M. (1994) *J. Biol. Chem.* **269**, 30125–30131.
11. Gautron, S., DosSantos, G., Pinto-Henrique, D., Koulakoff, A., Gros, F. & Bewald-Netter, Y. (1992) *Proc. Natl. Acad. Sci. USA* **89**, 7272–7276.
12. Gellens, M. E., George, A. L., Jr., Chen, L. Q., Chahine, M., Horn, R., Barchi, R. L. & Kallen, R. G. (1992) *Proc. Natl. Acad. Sci. USA* **89**, 554–558.
13. George, A. L., Jr., Knittle, T. J. & Tamkun, M. M. (1992) *Proc. Natl. Acad. Sci. USA* **89**, 4893–4897.
14. Kallen, R. G., Sheng, Z. H., Yang, J., Chen, L. Q., Rogart, R. B. & Barchi, R. L. (1990) *Neuron* **4**, 233–242.
15. Kayano, T., Noda, M., Flockerzi, V., Takahashi, H. & Numa, S. (1988) *FEBS Lett.* **228**, 187–194.
16. Klugbauer, N., Lacinova, L., Flockerzi, V. & Hofmann, F. (1995) *EMBO J.* **14**, 1084–1090.

17. Noda, M., Ikeda, T., Kayano, T., Suzuki, H., Takeshima, H., Kurasaki, M., Takahashi H. & Numa, S. (1986) *Nature (London)* **320**, 188–192.
18. Noda, M. & Numa, S. (1987) *J. Recept. Res.* **7**, 467–497.
19. Rogart, R. B., Cribbs, L. L., Muglia, L. K., Kephart, D. & Kaiser, M. W. (1989) *Proc. Natl. Acad. Sci. USA* **86**, 8170–8174.
20. Sangameswaran, L. B., Delgado, S. G., Fish, L. M., Koch, B. D., Jakeman, L. B., Stewart, G. R., Sze, P., Hunter, J. C., Eglén, R. M. & Herman, R. C. (1996) *J. Biol. Chem.* **271**, 5953–5956.
21. Trimmer, J. S., Cooperman, S. S., Tomiko, S. A., Zhou, J. Y., Crean, S. M., Boyle, M. B., Kallen, R. G., Sheng, Z. H., Barchi, R. L., Sigworth, F. J., Goodman, R. H., Agnew, W. S. & Mandel, G. (1989) *Neuron* **3**, 33–49.
22. Schaller, K. L., Krzemien, D. M., Yarowsky, P. J., Krueger, B. K. & Caldwell, J. H. (1995) *J. Neurosci.* **15**, 3231–3242.
23. Toledo-Aral, J. J., Moss, B. L., He, Z. J., Koszowski, A. G., Whisenand, T., Levinson, S. R., Wolf, J. J., Silos-Santiago, I., Halegoua, S. & Mandel, G. (1997) *Proc. Natl. Acad. Sci. USA* **94**, 1527–1532.
24. Yarowsky, P. J., Krueger, B. K., Olson, C. E., Clevinger, E. C. & Koos, R. D. (1991) *Proc. Natl. Acad. Sci. USA* **88**, 9453–9457.
25. Yarowsky, P. J., Krueger, B. K., Olson, C. E., Clevinger, E. C. & Koos, R. D. (1992) *Proc. Natl. Acad. Sci. USA* **89**, 3669.
26. Catterall, W. A. (1988) *Science* **242**, 50–61.
27. Goldin, A. L. (1993) *Curr. Opin. Neurobiol.* **3**, 272–277.
28. Isom, L. L., De Jongh, K. S. & Catterall, W. A. (1994) *Neuron* **12**, 1183–1194.
29. Isom, L. L., De Jongh, K. S., Patton, D. E., Reber, B. F., Offord, J., Charbonneau, H., Walsh, K., Goldin, A. L. & Catterall, W. A. (1992) *Science* **256**, 839–842.
30. Numann, R., Catterall, W. A. & Scheuer, T. (1991) *Science* **254**, 115–118.
31. West, J. W., Patton, D. E., Scheuer, T., Wang, Y., Goldin, A. L. & Catterall, W. A. (1992) *Proc. Natl. Acad. Sci. USA* **89**, 10910–10914.
32. Li, M., West, J. W., Lai, Y., Scheuer, T. & Catterall, W. A. (1992) *Neuron* **8**, 1151–1159.
33. Rudy, B., Vega-Saenz de Miera, E., Sugimori, M. & Llinás, R. (1994) *Soc. Neurosci. Abstr.* **20**, 64.
34. Lambolez, B., Audinat, E., Bochet, P., Crepel, F. & Rossier, J. (1992) *Neuron* **9**, 247–258.
35. Anderson, P. A. V., Holman, M. A. & Greenberg, R. M. (1993) *Proc. Natl. Acad. Sci. USA* **90**, 7419–7423.
36. Sato, C. & Matsumoto, G. (1992) *Biochem. Biophys. Res. Commun.* **186**, 61–68.
37. Rosenthal, J. J. & Gilly, W. F. (1993) *Proc. Natl. Acad. Sci. USA* **90**, 10026–10030.
38. Ramaswami, M. & Tanouye, M. A. (1989) *Proc. Natl. Acad. Sci. USA* **86**, 2079–2082.
39. Salkoff, L., Butler, A., Scavarda, N. & Wie, A. (1987) *Nucleic Acids Res.* **15**, 8569–8572.
40. Vega-Saenz de Miera, E. C. & Jen-Wei, L. (1992) *Methods Enzymol.* **207**, 613–619.
41. Mead, D. A., Pey, N. K., Herrnstadt, C., Marcil, R. A. & Smith, L. M. (1991) *Bio/Technology* **9**, 657–663.
42. Sanger, F., Nicklen, S. & Coulson, A. R. (1977) *Proc. Natl. Acad. Sci. USA* **74**, 5463–5467.
43. Feinberg, A. & Vogelstein, B. (1983) *Analyt. Biochem.* **132**, 6–13.
44. Chomczynski, P. & Sacchi, N. (1987) *Analyt. Biochem.* **162**, 156–159.
45. Rudy, B., Hoger, J. H., Lester, H. A. & Davidson, N. (1988) *Neuron* **1**, 649–658.
46. Stone, D. M., Wessel, T., Joh, T. H. & Baker, H. (1990) *Mol. Brain Res.* **8**, 291–300.
47. Paxinos, G. (1995) *The Brain Nervous System* (Academic, New York), 2nd Ed.
48. Paxinos, G. & Watson, C. (1986) *The Rat Brain in Stereotaxic Coordinates* (Academic, Orlando, FL), 2nd Ed.
49. Swanson, L. W. (1992) *Brain Maps: Structure of the Rat Brain* (Elsevier, New York).
50. Vega Saenz de Miera, E., Weiser, M., Kentros, C., Lau, D., Moreno, H., Serodio, P. & Rudy, B. (1994) in *Handbook of Membrane Channels* (Academic, New York), pp. 41–78.
51. George, A. L., Jr., Iyer, G. S., Kleinfeld, R., Kallen, R. G. & Barchi, R. L. (1993) *Genomics* **15**, 598–606.
52. Loughney, K., Kreber, R. & Ganetzky, B. (1989) *Cell* **58**, 1143–1154.
53. McClatchey, A. I., Lin, C. S., Wang, J., Hoffman, E. P., Rojas, C. & Gusella, J. F. (1993) *Hum. Mol. Genet.* **1**, 521–527.
54. French, C. R., Sah, P., Buckett, K. J. & Gage, P. W. (1990) *J. Gen. Physiol.* **95**, 1139–1157.
55. Moorman, J. R., Kirsch, G. E., VanDongen, A. M. J., Joho, R. H. & Brown A. M. (1990) *Neuron* **4**, 243–252.
56. Burgess, D. L., Kohrman, D. C., Galt, J., Plummer, N. W., Jones, J. M., Spear, B. & Meisler, M. H. (1995) *Nat. Genet.* **10**, 461–465.
57. Kohrman, D. C., Harris, J. B. & Meisler, M. H. (1996) *J. Biol. Chem.* **271**, 17576–17581.
58. Harris, J. B., Boakes, R. J. & Court, J. A. (1992) *J. Neurol. Sci.* **110**, 186–194.
59. Kohrman, D. C., Smith, M. R., Goldin, A. L., Harris, J. & Meisler, M. H. (1996) *J. Neurosci.* **16**, 5993–5999.
60. Dick, D. J., Boakes, R. J., Candy, J. M., Harris, J. B. & Cullen, M. J. (1986) *J. Neurol. Sci.* **76**, 255–267.